ISBN 82-553-0363-4

Applied Mathematics
No 4 - November 13 1978

# A NUMERICAL MODEL FOR LONG BAROTROPIC WAVES AND STORM SURGES ALONG THE WESTERN COAST OF NORWAY

by

E.A. Martinsen, B. Gjevik
and L.P. Røed
Oslo

PREPRINT SERIES - Matematisk institutt, Universitetet i Oslo

# A NUMERICAL MODEL FOR LONG BAROTROPIC WAVES AND STORM SURGES ALONG THE WESTERN COAST OF NORWAY

by

E.A. Martinsen, Department of Mathematics, Univ. of Oslo, Norway
B. Gjevik, Department of Mathematics, Univ. of Oslo, Norway
L.P. Röed, Geophysical Institute, Div.A., Univ. of Bergen, Norway

## Abstract

A finite difference scheme is used in order to study the generation and propagation of long barotropic waves and storm surges along the western coast of Norway. The performance of the numerical scheme is investigated by comparing with analytical solutions for a model with a straight coastline and a continental shelf of uniform depth and width. Simulations with a model of the west coast of Norway show that the wind stress and the atmospheric pressure are of about equal importance for the large storm surges. The maximum elevation of the sea surface occurs at the coast and the sea level decreases nearly linearly over the shelf. The surge amplitude at the coast agrees well with observations. The sea level changes outside the shelf are small and for the most part due to the pressure. Shelf waves are mainly generated by the wind stress, and Kelvin waves are mainly generated by the pressure field.

## 1. INTRODUCTION

Changes in sea level and currents induced by wind stress and air pressure have been the subject of numerous studies. In particular there has been made a considerable effort to develop methods which enable forcasting of storm surges. Reviews of the literature has been given by Bretschneider (1967).

Along a coast with a relatively narrow shelf, long barotropic waves trapped to the shelf or the coastal boundary play an important role for sea level changes and currents. The dynamics of these waves have been studied in many papers especially in the last decade, and the general properties of these waves are now well known (Le Blond and Mysak, 1978). Most of the theoretical studies have been concerned with very idealized conditions where bottom topography as well as the atmospheric forcing are represented by simple models. For that reason it will be of general interest to investigate the generation and propagation of long barotropic waves in cases where the bottom topography and the atmospheric forcing are given more realistic representations.

The present activity on the Norwegian shelf requires more knowledge of the sea level variations and the currents that are induced by travelling weather systems. In this study we have therefore modeled the western coast of Norway. Storm surges in this area were first studied by Gjevik and Röed (1976), and the maximum sea elevation due to atmospheric effects along this coast is of the order 1.5 - 2.0 m Gjevik (1978). Martinsen (1978) used a numerical model for sea level variations along the western coast of Norway and demonstrated that the topography of the shelf had an important effect.

In this study we will refine his numerical model, and simulate different weather situations. We will also compare numerical and analytical solutions for a simple step-shelf model. This gives a check on the performance of the numerical scheme. Moreover the results for the step-shelf model enable us to see how the response of the ocean is modified when the bottom topography is more complex.

## 2. BASIC EQUATIONS AND NUMERICAL PROCEDURE

Since we are interested in the barotropic response of the ocean to disturbances of large horizontal extent compared to the depth we shall use the linearized, depth integrated shallow water equations for an inviscid fluid. In a Cartesian coordinate system with horizontal axis $x$ and $y$ these equations can be written

$$\frac{\partial U}{\partial t} - fV = - c^2 \frac{\partial \eta}{\partial x} - \frac{h}{\rho_s} \frac{\partial p}{\partial x} + \frac{1}{\rho_s} \tau_x \,, \tag{2-1}$$

$$\frac{\partial V}{\partial t} + fU = - c^2 \frac{\partial \eta}{\partial y} - \frac{h}{\rho_s} \frac{\partial p}{\partial y} + \frac{1}{\rho_s} \tau_y \,, \tag{2-2}$$

and

$$\frac{\partial \eta}{\partial t} = - \frac{\partial U}{\partial x} - \frac{\partial V}{\partial y} \,. \tag{2-3}$$

Here $U$ and $V$ denote respectively the volume flux in the $x$ and $y$ direction; $\eta$ is the elevation of the sea surface above the equilibrium level; $\tau_x$ and $\tau_y$ are the $x$ and $y$ components of the wind stress acting on the sea surface, $p$ the atmospheric pressure at the sea surface, $\rho_s$ is a mean density of sea water; $h$ is the depth; $c^2 = gh$, where $g$ is the acceleration due to gravity; and $f$ is the Coriolis parameter. Since the friction at the bottom is

of minor importance for the flow phenomena that we will study (See section 4), terms which should represent the bottom stress is neglected in eqs. (2-1) - (2-2).

The coast is thought to be impermeable and no flow perpendicular to the coast is therefore permitted. Hence if $\mathbf{n}$ denotes the unit vector normal to the coast and $\mathbf{U}$ the flux vector $\{U,V\}$, the boundary condition at the coastline can be written

$$\mathbf{U} \cdot \mathbf{n} = 0 \ . \tag{2-4}$$

Since we will study flow phenomena confined to a limited region along the coast we will also use the open boundary condition $\eta \to 0$ at boundaries far away from this region.

The wind stress is related to the atmospheric pressure disturbance and we will use a simplified model for simulating this relationship. A propagating pressure disturbance is described by

$$p = p_0(t)\ e^{-[(x-x_0-u_0t)^2 + (y-y_0-v_0t)^2]/R^2} \tag{2-5}$$

where $p_0$ is a function of time; $x_0$, $y_0$ is the initial position of the center of the pressure disturbance; $u_0$ and $v_0$ are the $x$ and $y$ components of the propagation velocity; and $R$ is a constant which defines the horizontal extent of the pressure disturbance.

The wind velocity components $u_g$ and $v_g$ respectively along the $x$ and $y$ directions are taken to be a fraction of the geostrophic wind components. Hence

$$u_g = - \frac{\sigma}{f\rho_a} \frac{\partial p}{\partial y} \ ,$$

$$v_g = \frac{\sigma}{f\rho_a} \frac{\partial p}{\partial x}$$

where $\rho_a$ is the density of the air and the ratio $\sigma$ is positive and less than unity. Asymptotic wind fields are simulated by choosing $\sigma$ as a function of $x$ and $y$.

The wind stress is related to the wind velocity by the empirical relations

$$\tau_x = \rho_a \, c_D (u_g^2 + v_g^2)^{\frac{1}{2}} \, u_g \,, \qquad (2\text{-}6)$$

$$\tau_y = \rho_a \, c_D (u_g^2 + v_g^2)^{\frac{1}{2}} \, v_g$$

where $c_D$ is the drag coefficient.

Eqs. (2-1) - (2-3) will be solved by a finite difference scheme and we will use a staggered grid for the discretization in space. The grid we use corresponds to lattice C, p.47, Mesinger and Arakawa (1976). In time we have used forward differences in the continuity equation (2-3) and backward differences in eqs. (2-1) - (2-2) except for the Coriolis term in eq. (2-1). This is done in order to obtain a numerically stable scheme even when the bottom friction terms are neglected. Heaps (1969), Sielecki (1968). A set of difference equations corresponding to eqs. (2-1) - (2-3) can be written

$$\eta_{x,y}^{t+\Delta t} = \eta_{x,y}^{t} - \gamma(\partial_x U_{x,y}^{t} + \partial_y V_{x,y}^{t}) \,,$$

$$U_{x,y}^{t+\Delta t} = U_{x,y}^{t} + f \, \Delta t \, \bar{V}_{x,y}^{t} - g h_{x,y} \gamma \, \partial_x \eta_{x,y}^{t+\Delta t} + \Delta t \, X_{x,y}^{t+\Delta t} \,, \qquad (2\text{-}7)$$

$$V_{x,y}^{t+\Delta t} = V_{x,y}^{t} - f \, \Delta t \, \bar{U}_{x,y}^{t+\Delta t} - g h_{x,y} \gamma \, \partial_y \eta_{x,y}^{t+\Delta t} + \Delta t \, Y_{x,y}^{t+\Delta t} \,,$$

where the upper and lower indices indicate respectively the time and space discretization. The operators $\partial_x$, $\partial_y$ and the averaging operator are defined by

$$\partial_x A_{x,y} = A_{x+\Delta s,y} - A_{x-\Delta s,y} ,$$

$$\partial_y A_{x,y} = A_{x,y+\Delta s} - A_{x,y-\Delta s} ,$$

$$\bar{A}_{x,y} = \frac{1}{4}[A_{x+\Delta s,y+\Delta s} + A_{x+\Delta s,y-\Delta s} + A_{x-\Delta s,y-\Delta s} + A_{x-\Delta s,y+\Delta s}] .$$

The time and space increments are $\Delta t$ and $\Delta s$, and $\gamma = \Delta t/2\Delta s$. In eq. (2-7) X and Y are taken to represent the forcing terms due to atmospheric pressure and wind stress at the surface of the sea. The staggered grid enables a simple representation of the boundary condition at the coastline since the coastline can be drawn along lines which only requires specification of either U or V.

The numerical stability of the homogeneous difference equations (2-7) can easily be done by a standard procedure, Mesinger and Arakawa (1976). We assume uniform depth and find that in order to obtain a stable scheme

$$\Delta t \leq \Delta s \sqrt{\frac{2}{gh}} \qquad (2\text{-}8)$$

The numerical dispersion and dissipation of free waves can be studied by a similar technique. We find that the numerical scheme has no numerical dissipation. Fig. 1 summarizes the dispersion for a model where the depth varies between 250 m and 2000 m. In these computations $\Delta t = 200$ s, $\Delta s = 2 \cdot 10^4$ m, $g = 10.0$ ms$^{-2}$, $f = 1.3 \cdot 10^{-4}$ s$^{-1}$. The time step corresponds to the largest time allowed by the stability condition

(2-8) with $h = 2000$ m. These results indicate that with this time step the numerical scheme will perform well for disturbances with length scale larger than say $8\Delta s$ in a model where the depth varies between 250 and 2000 m.

## 3. ANALYTICAL AND NUMERICAL SOLUTIONS FOR A STEP-SHELF MODEL.

Fig. 2 shows the bottom topography and coastline for the step-shelf model. The sea is of uniform depth; $H_0$ on the shelf and $H_1$ off the shelf. The width of the shelf is $L$ and the coastline is straight.

The dispersion properties of free waves in this model have been investigated by Munk, Snodgrass and Wimbush (1970). When the forcing terms in eqs. (2-1) and (2-2) are omitted, we assume solutions of the form

$$\{U,V,\eta\} = \{U',V',\eta'\}e^{ik(x-ct)}$$

where $U'$, $V'$ and $\eta'$ are functions of $y$ only. The wave number $k$ and the phase speed $c$ are constants. The boundary conditions, $\eta \to 0$ for $y \to \infty$, $V$ and $\eta$ continuous at $y = 0$, and $V = 0$ at $y = -L$, lead to the relation

$$\tanh(\alpha_0 L) = \frac{c\alpha_0(f-c\alpha_1)}{f(f-c\alpha_1)-(f^2-c^2\alpha_0^2)\frac{c_0^2}{c_1^2}} \qquad (3\text{-}1)$$

where

$$c_0 = \sqrt{gH_0}\ ,$$

$$c_1 = \sqrt{gH_1}\ ,$$

$$c_0\alpha_0 = \sqrt{f^2+(c_0^2-c^2)k^2} \ ,$$

$$c_1\alpha_1 = \sqrt{f^2+(c_1^2-c^2)k^2} \ .$$

Eq.(3-1) determines the dispersion relation for free waves. For low frequency waves $kc < f$, only two trapped modes are possible. These wave modes are the shelf wave and the Kelvin type edge wave and the dispersion relations for $\frac{c_0}{c_1} = 0.35$ and $\frac{fL}{c_0} = 0\ 55$ are depicted in fig. 3. The values of the parameters which characterize the step-shelf model are representative for the shelf along the western coast of Norway.

In order to investigate the performance of the numercial scheme we have studied the propagation of the shelf wave mode and the edge wave mode for the same step-shelf model as above. Analytical expressions for these modes are used in order to generate initial conditions for the numerical integration. In this experiment the shelf width is 10.5 $\Delta s$. By integrating numerically over a time span $t_s$ corresponding to $ft_s = 8$ a mean propagation velocity for the waves can be found. This has been done for different wave lengths and the results are shown in fig. 3. For $0 < kL < 1.5$ we conclude that the numerical model gives values of the propagation velocity for the shelf wave mode which is within 15% of the correct value. For the Kelvin edge wave mode the agreement is better (3%). We believe that the averaging of the Coriolis terms in eqs. (2-7) introduces errors for the shelf wave mode.

For the step-shelf model also a forced solution of eqs. (2-1) - (2-3) can be found analytically. We will examine a case where the

wind stress decays exponentially off the coast. It is acting along the direction of the coastline, and hence we put

$$\tau_x = \rho_s \tau_0(x,t) e^{-\alpha(y+L)} , \qquad \tau_y = 0 \tag{3-2}$$

where $\tau_0(x,t)$ is a function of $x$ and $t$ which will be specified at a later stage and $\alpha$ is a constant. We define the Laplace and Fourier-transforms of a function $\varphi$ of $x$ and $t$ by

$$\tilde{\varphi} = \int_0^{\infty} \varphi \, e^{-st} \, dt ,$$

$$\bar{\varphi} = \int_{-\infty}^{+\infty} \varphi \, e^{-ikx} \, dx .$$

Assuming that the Laplace and Fourier transforms exist with a particular choice of the function $\tau_0$ the transformation of eqs. (2-1) - (2-3) leads to

$$\frac{d^2\tilde{\bar{\eta}}}{dy^2} = \beta^2 \tilde{\bar{\eta}} + \left(\frac{iks+f\alpha}{c^2 s}\right) \tilde{\bar{\tau}}_0 \, e^{-\alpha(y+L)} , \tag{3-3}$$

$$\tilde{\bar{V}} = \frac{1}{s^2+f^2}\left[ c^2 \left( ifk\tilde{\bar{\eta}} - s \frac{d\tilde{\bar{\eta}}}{dy} \right) - f \, \tilde{\bar{\tau}}_0 e^{-\alpha(y+L)} \right] \tag{3-4}$$

where

$$\beta^2 = \frac{s^2+f^2+c^2k^2}{c^2} .$$

For $-L < y < 0$: $c = c_0$, $\beta = \beta_0$ and for $y > 0$: $c = c_1$, $\beta = \beta_1$

The initial value of $U$, $V$ and $\eta$ are taken to be zero. The integration constants of (3-3) are determined by the boundary conditions $\tilde{\bar{\eta}} \to 0$ for $y \to \infty$, $\tilde{\bar{V}} = 0$ for $y = -L$ and $\tilde{\bar{\eta}}$ and $\tilde{\bar{V}}$

continuous at $y = 0$. The resulting expression for $\tilde{\eta}$ becomes rather involved and in order to obtain an attractable expression for $\tilde{\eta}$, which in turn can be inverted, we introduce some simplifications. We assume that the wind stress has a longshore extent much larger that L and that the energy containing part of the spectrum of $\tau_0$ consists of waves with lengths much larger than the shelf width. This justifies to use $kL << 1$ as an expansion parameter. We also assume that the deformation radius $c_0/f$ is much larger than the shelf width, i.e. $\frac{fL}{c_0} << 1$. Moreover, we assume $\frac{c_0^2}{c_1^2} << 1$ and will consider solutions valid for times larger than the inertial period. These assumptions correspond to those used by Gill and Schumann (1974) and a discussion of the validity of these assumptions can also be found in their paper.

By involing the assumtions above, we obtain when only the most significant terms are retained

$$\tilde{\eta} = 0 , \qquad \text{for } y = 0 , \tag{3-5}$$

$$\tilde{\eta} = \frac{fL}{c_0} \frac{\tilde{\tau}_0}{c_0} \frac{q}{s+ikfL} , \qquad \text{for } y = -L \tag{3-6}$$

where

$$q = (1 - e^{-\alpha L})/\alpha L .$$

In the interval $(-L,0)$ $\tilde{\eta}$ varies nearly linearly with y.

We will invert the expression (3-6) for a particular choice of the function $\tau_0$, viz.,

$$\tau_0(x,t) = \tau_m e^{-\kappa^2 x^2} h(t) \tag{3-7}$$

where $h(t)$ is the Heaviside unit step function, and $\tau_m$ and $\kappa$ are constants. The function (3-7) possesses the simple Laplace and Fourier transform

$$\tilde{\tau}_0 = \frac{\tau_m}{s} \frac{\sqrt{\pi}}{\kappa} e^{-\frac{k^2}{4\kappa^2}}$$

The inverted expression for the elevation of the sea surface at the coast (i.e. $\eta_L = \eta(x,y=-L,t)$) thus becomes

$$\eta_L(x,t) = q\eta_s\left[\operatorname{erf}(\kappa x) - \operatorname{erf}\kappa(x-fLt)\right] \qquad (3\text{-}8)$$

where

$$\eta_s = \frac{\tau_m\sqrt{\pi}}{2\kappa c_0^2}$$

and erf denotes the error function

$$\operatorname{erf} z = \frac{2}{\sqrt{\pi}} \int_0^z e^{-r^2} dr \ .$$

The solution (3-8) consists of two terms: a forced solution and a non-dispersive group of free shelf waves propagating along the coast with velocity $fL$.

To the order of approximation considered here there is no Kelvin edge wave excited by the wind stress.

Eq. (3-8) shows that the wind field generates an elevation of the sea surface which is confined essentially to the region of the shelf in front of the location of the maximum wind speed. Due to traveling shelf-waves the region with elevated sea level is expanding longshore with a velocity $fL$ in the x-direction. The elevation of the sea surface has its maximum value on the coast and the elevation decreases

nearly linearly toward zero at the outer edge of the shelf. By utilizing (3-8) the surface elevation due to constant wind stress of duration $T$ can be written down immediately. For $t$ somewhat larger than $T$ the surface elevation is made up of free shelf waves and the expression for the surface elevation at the coast is

$$\eta_L(x,t) = q\,\eta_s \left[\operatorname{erf}\kappa\,(x-fL(t-T)) - \operatorname{erf}\kappa\,(x-fLt)\right].$$

The maximum surface elevation at the coast is

$$2\,q\,\eta_s \operatorname{erf}\left(\frac{\kappa f L T}{2}\right).$$

The surface elevation corresponding to a steady wind stress of the form (3-7) moving in the x-direction with constant velocity, $u_0$, can also be expressed in terms of the error function. If $u_0 = fL$, i.e. the velocity of the shelf waves, resonance occurs and the surface elevation at the coast can be written

$$\eta_L(x,t) = 2\,q\,\eta_s \frac{\kappa L}{\sqrt{\pi}}\, ft\, e^{-\kappa^2(x-fLt)^2}$$

In order to obtain large surface elevation by resonance the wind stress has, however, to move along the coast for a considerable distance.

For a step-shelf model with $c_0/c_1 = 0.35$ and $fL/c_0 = 0.55$, we have integrated eqs. (2-7) numerically with a stationary wind forcing given by (3-7). The width of the shelf is taken to be $10.5\,\Delta s$. The initial values of the surface elevation and the volum fluxes are equal to zero. The results of the numerical integration in two cases are presented here. The contours for the elevation of the sea surface are depicted in the fig. 4 for the case $\alpha = 0$,

$\kappa = 1/5L$ and in fig. 5 for the case $\alpha = 1/L$ and $\kappa = 1/5L$.

These figures show that the region with the largest surface elevation is confined to the shelf. On fig. 4 the front of the disturbance extends off the shelf and propagates along the coast with a higher velocity than the rest of the disturbance. The high propagation velocity and the large extent perpendicular to the coast show that the disturbance consists of Kelvin type edge waves. The amplitude of these waves are, however, small compared to the amplitude of the shelf waves which are responsible for the main part of the surface elevation. In fig. 5 which shows the surface elevation for a wind field which decays exponentially in the direction perpendicular to the coast the edge wave mode is almost absent. The disturbance is essentially made up of a forced disturbance and free propagating shelf waves. This result is in agreement with the analytical results of eq. (3-8). By comparing the results of eq. (3-8) with the results of the numerical integration we also find that the eq. (3-8) gives the longshore extent of the region with surface elevation with a good degree of approximation for values of the time larger than 2/f. The maximum surface elevation at the coast differs by less than 25 % from values obtained by numerical integration. When eq. (3-8) was derived several approximations was made, but the errors are difficult to estimate. For that reason eq. (3-8) cannot be used to determine the accuracy of the numerical integration. For a model with uniform depth an exact solution for the sea elevation at the coast is available (Gjevik and Röed, 1976). In this case a numerical solution based on (2-7) is within 2 % of the corresponding analytical solution.

The case when the wind stress is acting in a direction normal to the coast is more difficult to examine analytically. Order of magnitude consideration (Gill and Schumann, 1974) shows that a wind stress acting normal to the coast generates considerably less surface elevation along the coast than a wind stress of similar strength acting in the direction of the coast.

We have integrated (2-1) - (2-3) numerically with the same bottom topography as above and with a wind stress

$$\tau_x = 0 \ , \qquad \tau_y = \rho \, \tau_0 (x,t) e^{-\alpha(y+L)}$$

where $\tau_0$ is given by (3-7).

For $\kappa = 1/5L$ and $\alpha = 1/2L$ the maximum surface elevation is about $0.3 \ \eta_s$. It is established at the coast after a relatively short time span $t = 1.3/f$. For larger values of $t$ the surface elevation at the coast decays. Oscillations in the surface elevation occur and the flow pattern is much more complex than in the cases shown in figures 4 and 5.

## 4. A NUMERICAL MODEL FOR THE WESTERN COAST OF NORWAY.

The main feature of the bottom topography and the coastline of this region is shown in fig. 6a. Fig. 6b shows the model of the bottom topography and the coastline which is used in most of our numerical studies. In this model only the main feature of the bottom topography is included and the depth is uniform on the shelf (250 m) and in the regions outside the shelf (2500 m). A more refined model of the bottom topography will modify the flow locally, but it will have minor effect on the large scale sea level variations on the shelf and along the coast. We will return to this point later.

The open boundary in the model is indicated by broken lines in fig. 6b and the distance from the coast to the boundary is shown by arrows.

In fig. 6b the track of the center of the pressure disturbance is shown for one of the cases which we have studied in detail. The initial position of the center together with the positions 12, 14 and 16 hours later are marked.

The pressure disturbance is of the form (2-5) and it is characterized by $R = 800$ km, $u_0 = 18.5\ ms^{-1}$ and $v_0 = -16.2\ ms^{-1}$ which implies that the speed of the center is $25\ ms^{-1}$. Initially $p_0 = 0$ and decreases smoothly to $p_0 = -50$ mb in 5.5 hours. This is done in order to avoid the gravity waves generated by rapid pressure variations.

The maximum wind speed occurs at a distance of 400 km from the center of the pressure disturbance and with $\sigma = 0.7$ which is used here, the maximum wind speed is $31\ ms^{-1}$. The track, speed and size of the pressure disturbance is chosen so that it simulates the cyclone of 2 November 1971. The induced surge combined with astronomic spring tide lead to unusual high sea level along the western coast of Norway. This situation is analysed by Gjevik and Röed (1976) and details on the surface pressure, wind and sea level variation can be found in their paper.

The following numerical values are used for the other parameters of the model $\Delta s = 10$ km, $\Delta t = 90$ s, $f = 1.3 \cdot 10^{-4} s^{-1}$, $g = 9.8\ ms^{-2}$ and $c_D = 3 \cdot 10^{-3}$.

In figure 7 the surface elevation due to the combined effect of pressure and wind stress is depicted for $t = 12$ hours, 14 hours and 16 hours. The three situations show that the largest surface elevation occurs at the coast and that the surface elevation outside the shelf has a much smaller value. On the shelf between Stad and Lofoten the contours of sea level run nearly parallel and they are equally spaced which shows that the sea level decreases nearly linearly over the shelf.

Northwest of Lofoten and in front of the region with the largest surface elevation we see that the contours for the sea level extend off the shelf. The picture of the surface elevation at 14 hours and 16 hours (fig. 7) show clearly how Kelvin edge waves are diffracted around the Northern coast of Norway and into the Barentz Sea. On the section of the coast between Stad and Lofoten the shelf waves are important, but it is difficult to estimate the amplitude of these shelf waves. In order to gain some insight into the process whereby the different wave modes are generated, we have calculated separately the effects of the wind stress and of the atmospheric pressure gradients. Figs. 8a and 8b show respectively the surface elevation at $t = 14$ hours due to these two different forcing mechanism. These figures show that in this case the wind stress and the pressure are of about equal importance. The horizontal extent of the elevated areas are, however, quite different in the two cases. The surface elevation generated by the pressure propagates into the Barentz Sea as Kelvin waves and along the edge toward Spitzbergen as double Kelvin waves. The double Kelvin waves can clearly be seen on plots subsequent to those in fig. 7. The main surface elevation generated by the wind stress is confined to the shelf and the form of the elevated area indicates that shelf waves are generated and that there is very little energy on the Kelvin edge wave mode in this case. Hence the wind stress seems to have the same effect as we found for the step-shelf model in section 3. The variation in the width of the shelf does, however, modify the motion in some respects. This is clearly seen on fig. 8c which displays the volume fluxes at 14 hours corresponding to the case depicted in

fig. 7. West of Stad the circulation along the outer edge of the shelf is clearly associated with shelf waves. The maximum volume fluxes occur north-west of Lofoten where the width of the shelf narrows in to about 40 km. The mean current velocity in this region is as high as 1.6 $ms^{-1}$ and this may partly be due to errors introduced by the numerical representation of the narrow shelf zone. It is, however, well known to fishermen that with the wind from south-west the current is extremely strong in this region. Measurements of the current velocity during storm situations like the one we simulated, is to our knowledge not available.

In fig. 9 we have displayed the computed sea level variation at two places on the coast namely: Kristiansund and Rörvik. The sea level variations due to atmospheric effects are estimated from the registrations of the sea level on 2 November 1972 and depicted in the same figure. It should be emphasized that the process whereby the sea level variations are estimated, introduces errors which may be of the order 0.2 m. The local topography in the vicinity of the recorder may also have a considerable effect on the recorded sea level. Having these effects in mind, we see that the computed and the observed sea elevation agree reasonably well. Comparison with observation at some other places is included in Table 1.

In order to investigate how the results are affected by bottom friction, asymmetry in the wind stress and changes in the bottom topography, we have made some simulations with these effects included in the model. Bottom friction effects are introduced by adding respectively the terms $-rU/h$ and $-rV/h$ to the right hand side of eqs. (2-1) and (2-2), and the friction coefficient $r$ is set to $2.4 \cdot 10^{-3} ms^{-1}$.

Table 1

| Location | Maximum surface elevation in meters | | | | |
|---|---|---|---|---|---|
| | Estimated from observations 2 Nov. 1971 | Computed values | | | |
| | | Basic model | Model with the Vøring plateau | Model with bottom friction | Model with asymmetric wind field |
| Kristiansund | 0.7 | 1.05 | 1.04 | 0.98 | 1.05 |
| Heimsjø | 1.0 | 1.16 | 1.16 | 1.08 | 1.16 |
| Rørvik | 1.4 | 1.51 | 1.56 | 1.40 | 1.50 |
| Sandnessjøen | 1.2 | 1.60 | 1.66 | 1.47 | 1.58 |
| Tromsø | 0.5 | 0.66 | 0.62 | 0.65 | 0.71 |

Asymmetric wind stress is simulated by $\sigma = 0.7(1-\frac{2}{3}\sin\varphi)$ for $0 < \varphi < \pi$ and $\sigma = 0.7$ for $\pi < \varphi < 2\pi$ where the angle $\varphi$ is defined in fig. 6b.

In the experiments with a refined bottom topography a plateau west of the shelf corresponding to the Vøring Plateau (see fig. 6a) is introduced in the model.

Some results of these computations are summarized in Table 1. We see that these refinements have only a minor effect on the maximum surface elevation along the coast. In other respects the changes in the model introduce some local modification. The Vøring Plateau will for example modify the flow pattern in its vicinity considerably. The reduction of the wind stress on the northern side of the track of the low pressure center reduces the outflow of water from the shelf north of Lofoten, and in Tromsø the maximum sea elevation will occur about 1 hour earlier than in the case of a symmetric wind stress.

We have also simulated two other weather situations. In the first case a pressure disturbance is moving in a north-easterly direction along a track which passes north of Norway. The south-westerly wind along the western coast of Norway has a maximum strength of about 25 $ms^{-1}$. The maximum surface elevation along the coast is found to be about 0.7 m. This simulation corresponds to the situation 30 December 1972 which is analysed by Gjevik and Röed (1976) and the computed surface elevation agrees well with observations. In this case the wind stress is the far most important mechanism for generating changes in sea level along the Norwegian coast.

In the second case a pressure disturbance is moving over land south of Stad and creates strong north-westerly winds (21 $ms^{-1}$) on

the coast between Stad and Lofoten. On this section of the coast where the wind stress is toward land, the surface elevation does not exceed 0.4 m and it is mainly due to the pressure effect. This result is therefore in agreement with the results for a step-shelf model which shows that a wind stress normal to the coast creates relatively small changes in sea level along the coast.

We have also made some studies in order to see how sensitive the results of the computations are to the grid size and to the position of the open boundaries. Experiments with the double grid size $\Delta s$ = 20 km, show that the surface elevation and the main features of the flow reproduced well. There will be some local distortion of the flow particularly in regions where the shelf is very narrow, and this does have some effect on flow in the region north-west of Lofoten. Experiments with the open boundaries further away from the coast show the same main features of the flow on the shelf. The modification of the maximum sea level at the coast in the 1971 case is less than 30 cm.

## 5. CONCLUDING REMARKS

It should be stressed that we so far have used simple models of the bottom topography and the atmospheric forcing when simulating sea level changes along the western coast of Norway. This is justified since we mainly want to demonstrate the dominant features of the barotropic response of the sea in this region. A more refined model of bottom topography and atmospheric forcing may have important local effects. In a refined model also the distance between the coast and the open boundaries need to be larger. The results of the preceeding section show, however, that the present model simulates the large scale features of the flow and the sea level variations, reasonably well.

ACKNOWLEDGEMENT

This work has been supported by Statoil, Det Norske Veritas and The Royal Norwegian Council for Scientific and Industrial Research (NTNF). The Norwegian Metorological Institute has provided us with free computer time.

REFERENCES

Bretschneider, C.L. (1967). Storm surges.(Advan. Hydrosci., 4, 341-418.

Gill, A.E. and Schumann, E.H. (1974). The generation of long shelf waves by the wind. J. Phys. Oceanogr., 4, 83-90.

Gjevik, B. (1978). Sea level changes along the coast of Norway. (In norwegian). Naturen, 4, 147-159, Universitetsforlaget, Oslo.

Gjevik, B. and Röed, L.P. (1976). Storm surges along the western coast of Norway. Tellus, vol. 28, No. 2, 166-182.

Heaps, N.S. (1969). A two-dimensional numerical sea model. Proc. R. Soc. Lond., A, 265, 93-137.

Le Blonde, P.H. and Mysak, L.A. (1978). Waves in the Ocean. Elsevier scientific publishing company, Amsterdam.

Martinsen, E.A. (1978). A numerical storm surge model related to the western coast of Norway. (In norwegian). Thesis work, University of Oslo.

Mesinger, F. and Arakawa, A. (1976). Numerical methods used in atmospheric models. GARP Publications series No. 17.

Munk, W.H., Snodgrass, F.E. and Wimbush, M. (1970). Tides off-shore: Transition from California coastal to deep-sea waters. Geophys. Fluid Dyn. 1, 161-235.

Sielecki, A. (1968). An energy-conserving difference scheme for storm surge equations. Mon. Weath. Rev., vol. 96, 150-156.

FIGURE CAPTIONS

Fig. 1 Dispersion relation for free waves. $k$ is the length of the wave number vector, $\omega$ is the frequency. Full drawn lines represent the dispersion relations for analytical wave solutions of eqs. (2-1)-(2-3) with a uniform depth $h = 250$ m and $h = 2000$ m. Broken lines represent dispersion relation for the difference equations (2-7). The direction of propagation relative to the x-axis is given in degrees.

Fig. 2 The geometry of the step-shelf model.

Fig. 3 Dispersion relation for trapped waves from eq. (3-1) for $c_0/c_1 = 0.35$ and $fL/c = 0.55$. The solid line represents the shelf wave mode and the broken line represents the Kelvin edge wave mode. Wave velocities obtained by numerical integration are marked with (x).

Fig. 4 Surface elevation for a step-shelf model and a wind stress given by eqs. (3-2) and (3-7) with $\kappa = 1/5L$ and $\alpha = 0$. The contours are in $\eta_s$ units, $c_0/c_1 = 0.35$ and $fL/c_0 = 0.55$. The outer edge of the shelf is marked by a dotted line.

Fig. 5 Surface elevation for the same model as in fig. 4, but with stress decaying in the direction normal to the coast, $\alpha = 1/L$.

Fig 6 a) Bottom topography of the sea west of Norway.

b) Geometry of the numerical model. The outer edge of the shelf is marked by a boken line - - - . The depth is 250 m on the shelf and 2500 m outside the shelf. The coastal boundary is drawn by a solid line. The open boundaries of the model is marked by a broken line -•-•-•- and the distance from the coast to these boundaries are shown by arrows.

The track of the low pressure center for one of the simulation experiments is shown, and the initial position of the center and the position of the center at 12, 14 and 16 hours are marked.

Maximum wind speed is along the circle.

Fig. 7 Sea elevation due to wind stress and pressure at t = 12, 14 and 16 hours. The unit for contours is in meter. The position of the center of the pressure disturbance is marked by L. The corresponding track of the center is shown in fig. 6 b.

Fig. 8 Sea elevation and volume fluxes at t = 14 hours for the same simulation as in fig. 7.

a) Sea elevation due to wind stress

b) Sea elevation due to pressure

c) Volume fluxes (combined effect of wind stress and pressure). The high fluxes north-west of Lofoten should be noted.

Fig. 9 Sea elevation at Kristiansund and Rörvik due to wind stress and pressure.

Solid line: computed values for the sea elevation.

Dotted line: values estimated from registrations 2 Nov 1971.

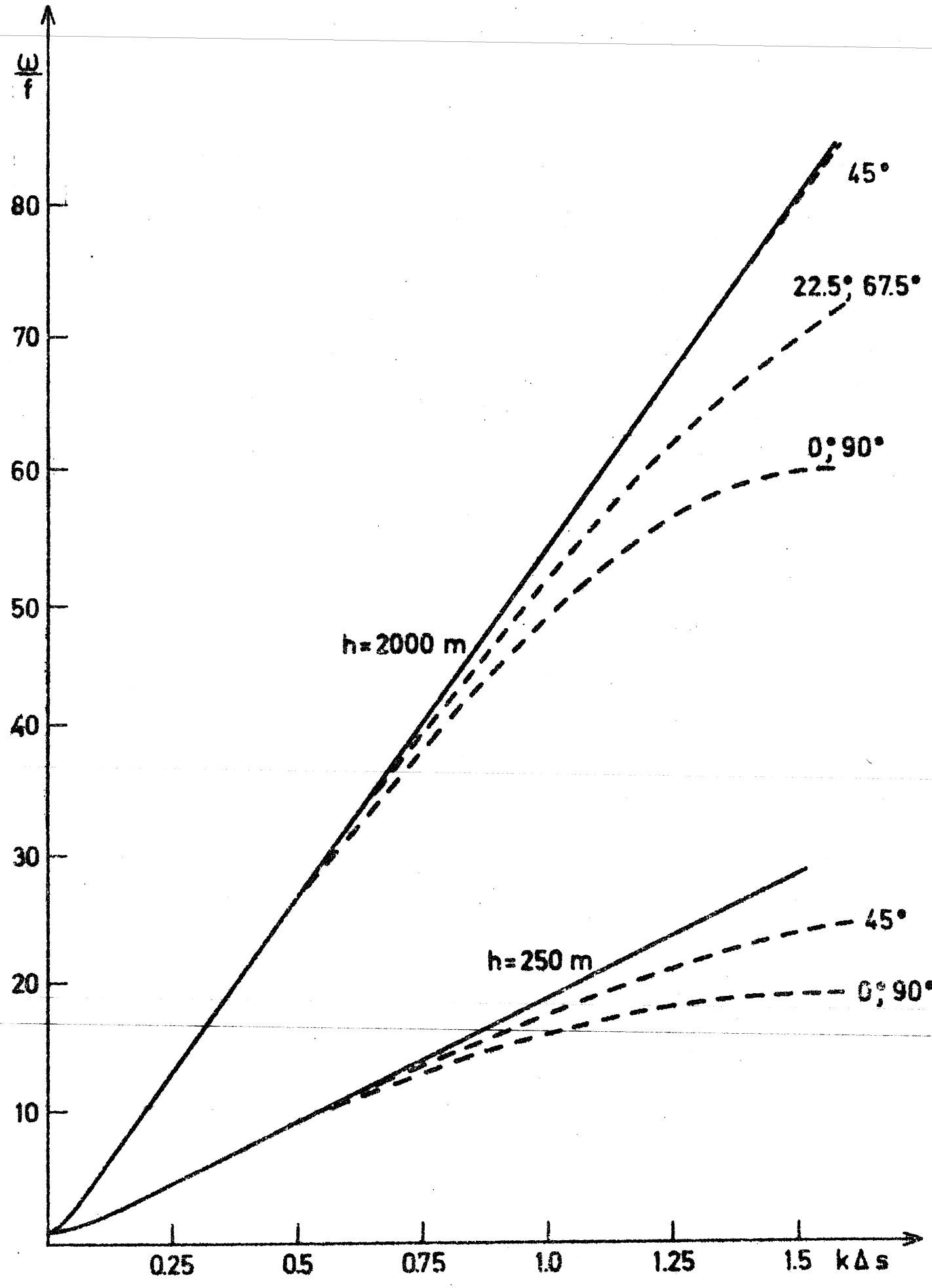
ω/f
80
70
60
50
40
30
20
10
45°
22.5°; 67.5°
0°; 90°
h=2000 m
45°
h=250 m
0°; 90°
0.25
0.5
0.75
1.0
1.25
1.5
kΔs

Fig. 1

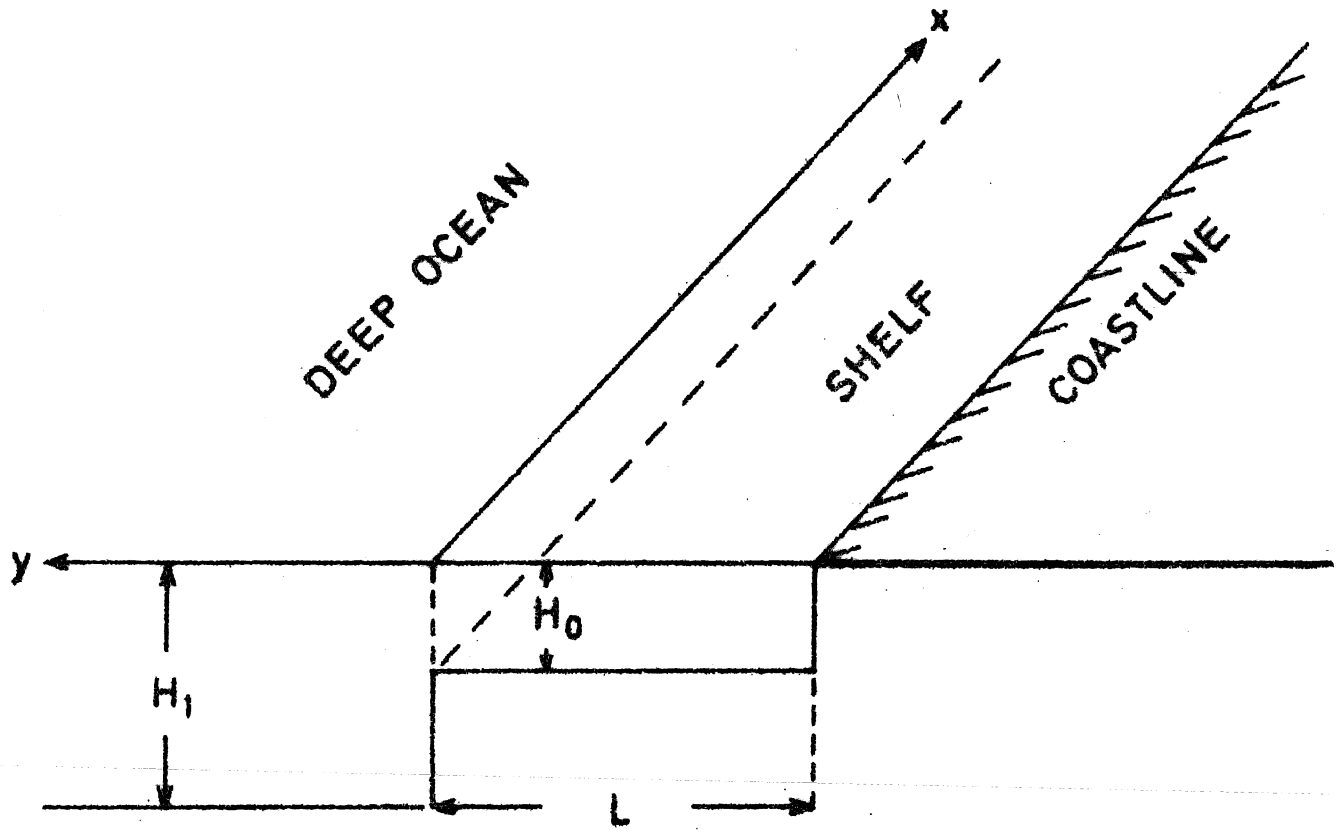


Fig. 2

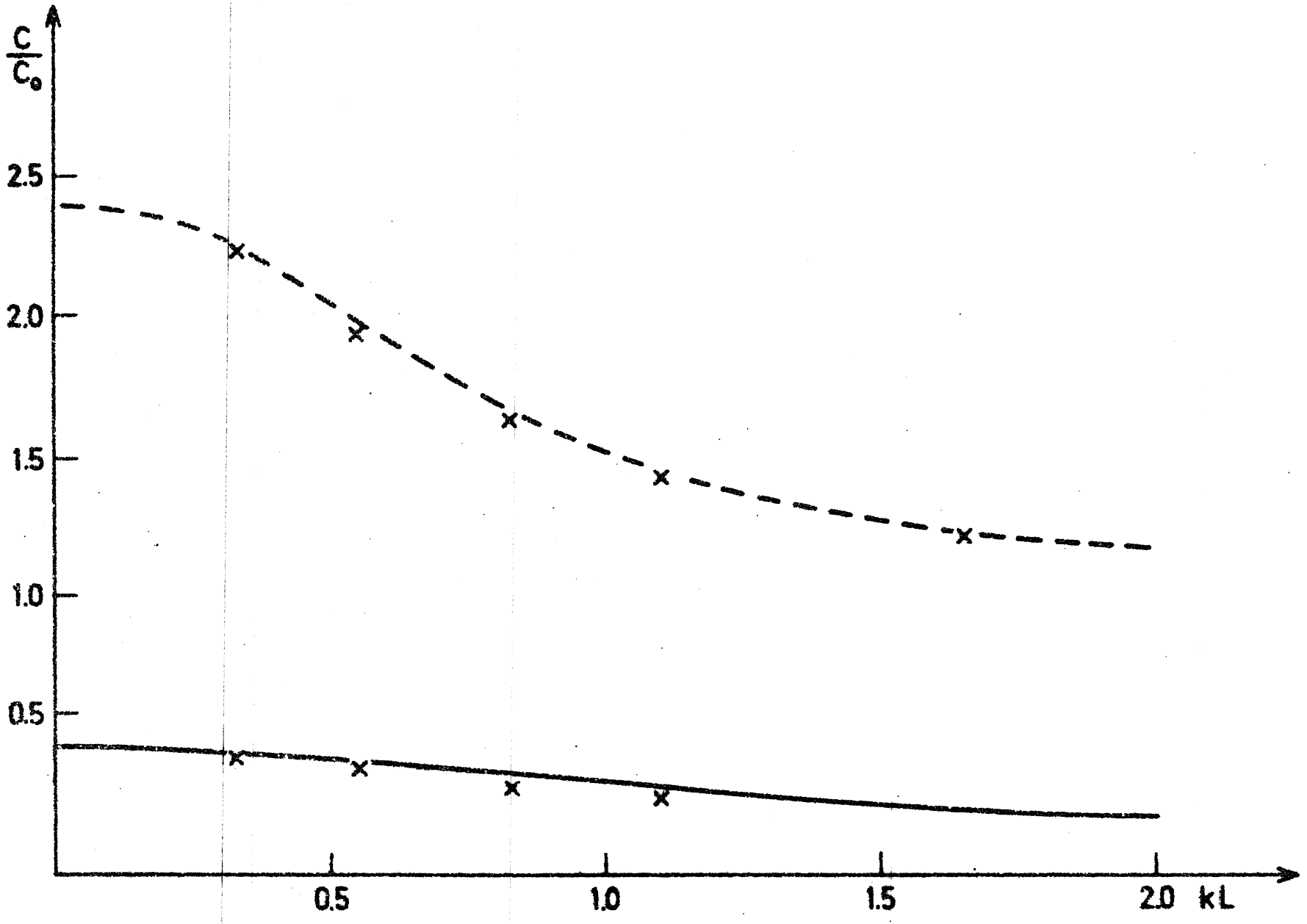


Fig. 3

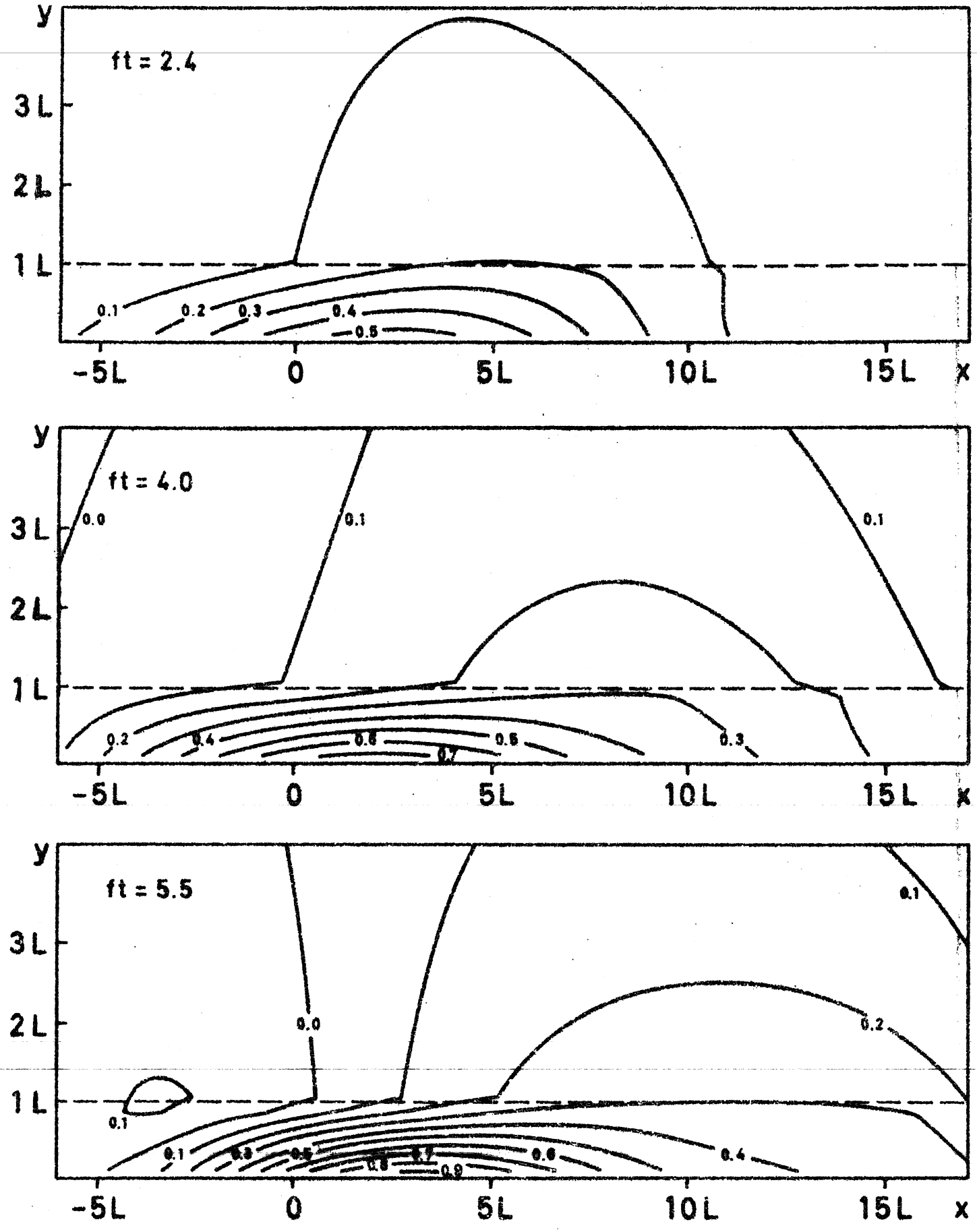
y
ft = 2.4
3L
2L
1L
0.1
0.2
0.3
0.4
0.5
-5L
0
5L
10L
15L
x
y
ft = 4.0
3L
2L
1L
0.0
0.1
0.1
0.2
0.4
0.6
0.5
0.7
0.3
-5L
0
5L
10L
15L
x
y
ft = 5.5
3L
2L
1L
0.1
0.0
0.2
0.1
0.3
0.5
0.6
0.7
0.8
0.9
0.4
-5L
0
5L
10L
15L
x

Fig. 4

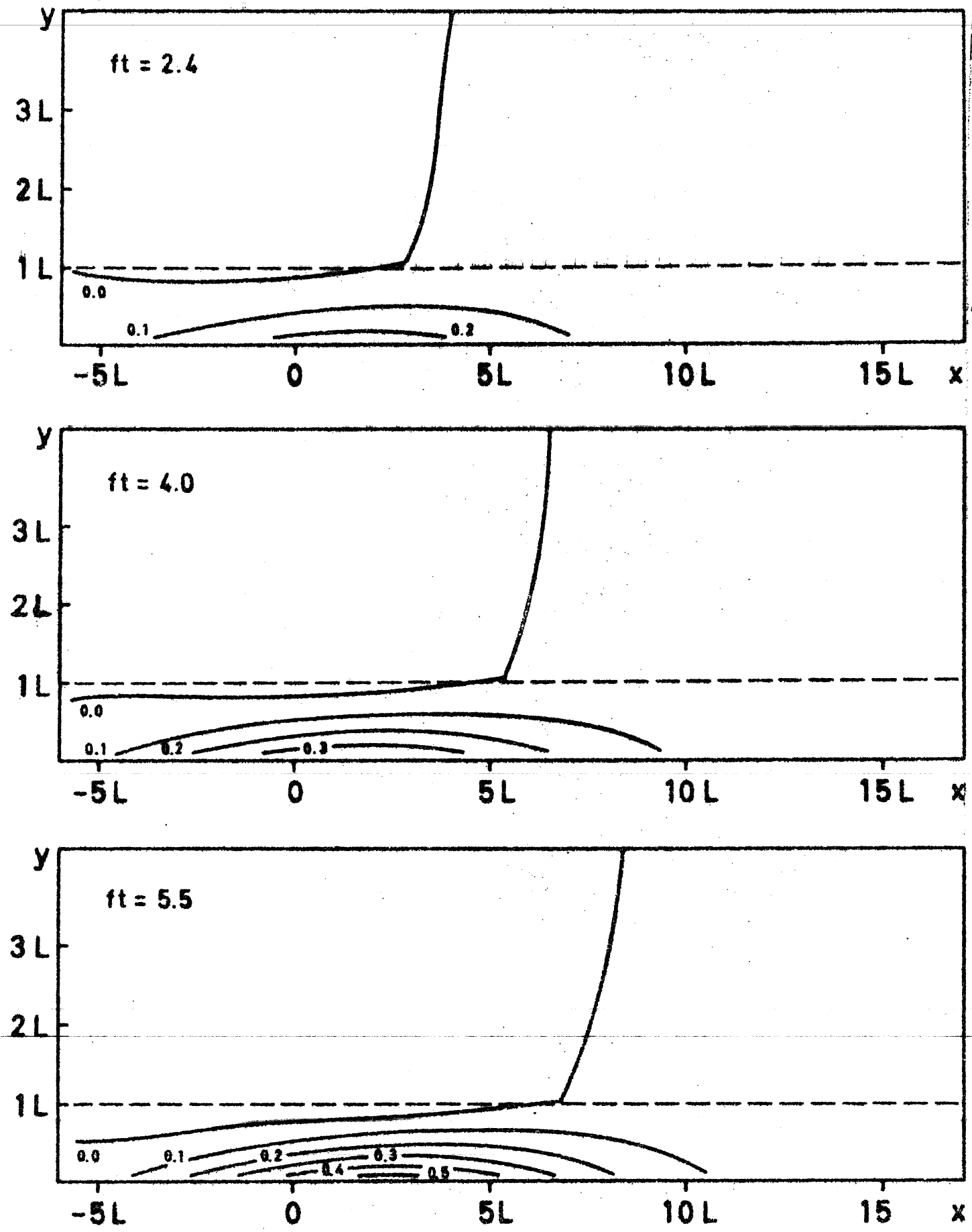
y
ft = 2.4
3L
2L
1L
0.0
0.1
0.2
-5L
0
5L
10L
15L
x
y
ft = 4.0
3L
2L
1L
0.0
0.1
0.2
0.3
-5L
0
5L
10L
15L
x
y
ft = 5.5
3L
2L
1L
0.0
0.1
0.2
0.3
0.4
0.5
-5L
0
5L
10L
15
x

Fig. 5

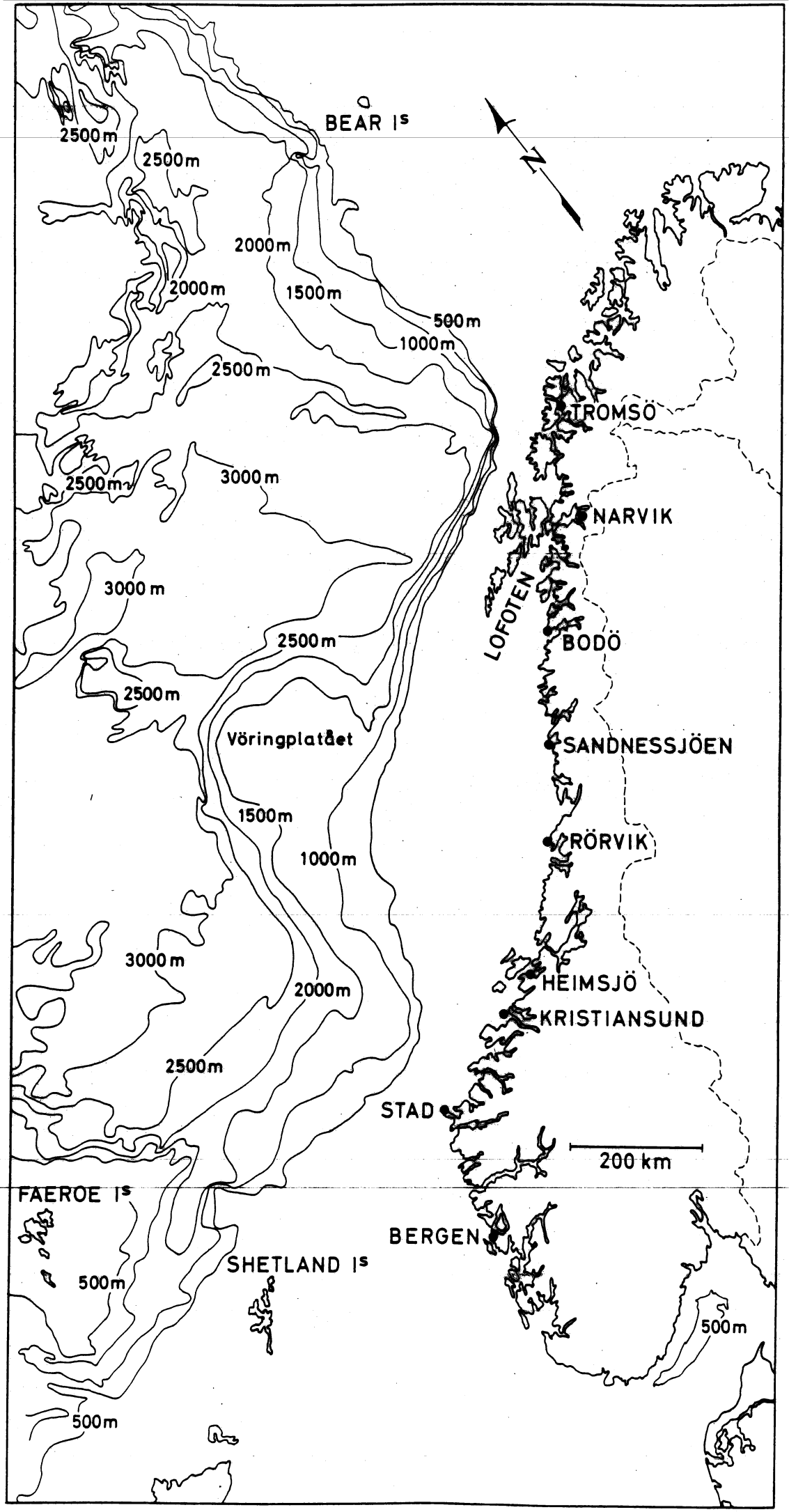
BEAR Is
N
2500m
2500m
2000m
2000m
1500m
500m
1000m
2500m
2500m
3000m
3000 m
2500m
2500m
Vöringplatået
1500m
1000m
3000m
2000m
2500m
TROMSÖ
NARVIK
LOFOTEN
BODÖ
SANDNESSJÖEN
RÖRVIK
HEIMSJÖ
KRISTIANSUND
STAD
200 km
FAEROE Is
SHETLAND Is
BERGEN
500m
500m
500m

Fig. 6a

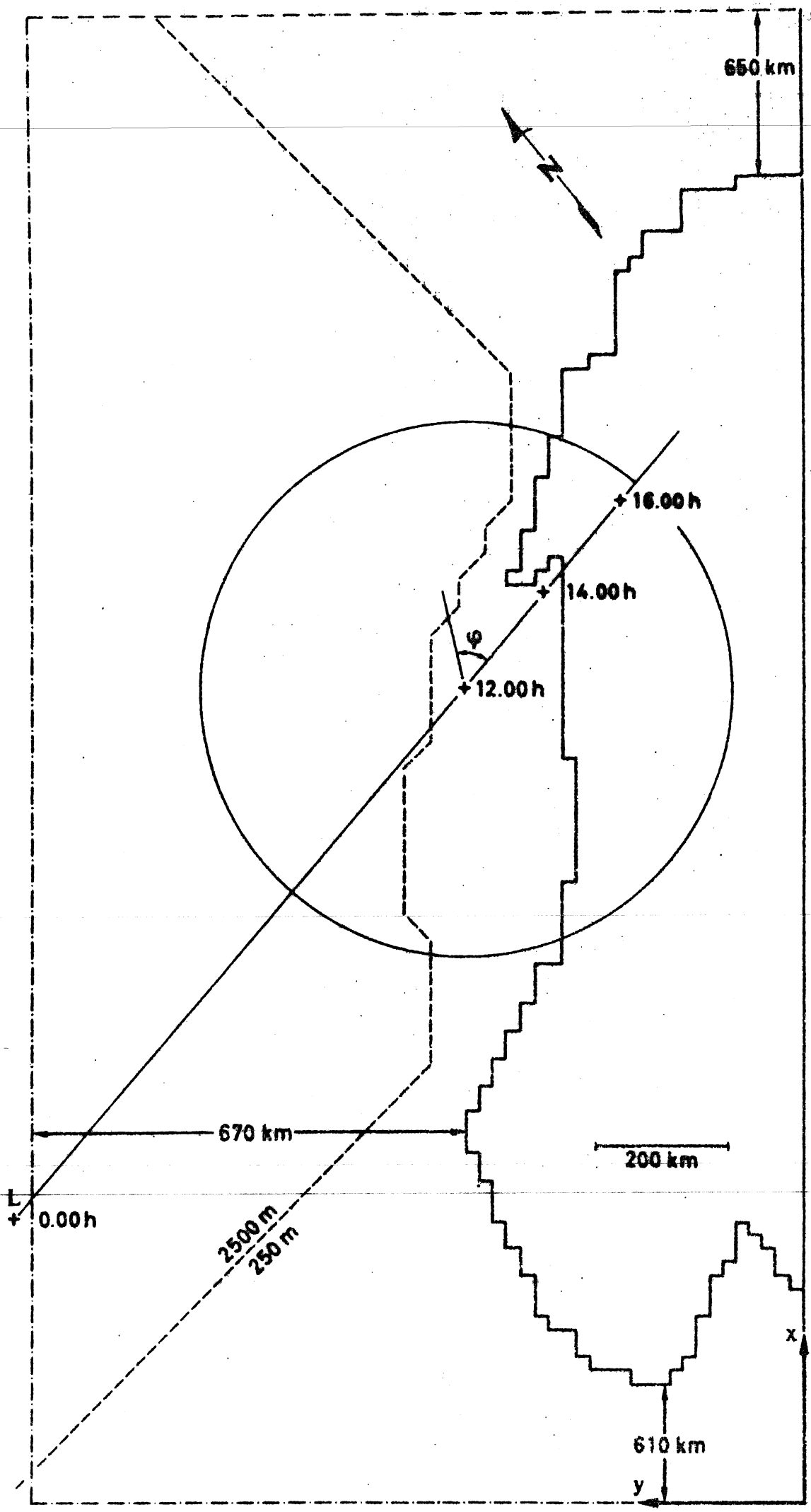
650 km
N
16.00 h
14.00 h
φ
12.00 h
670 km
200 km
L
0.00 h
2500 m
250 m
x
610 km
y

Fig. 6b

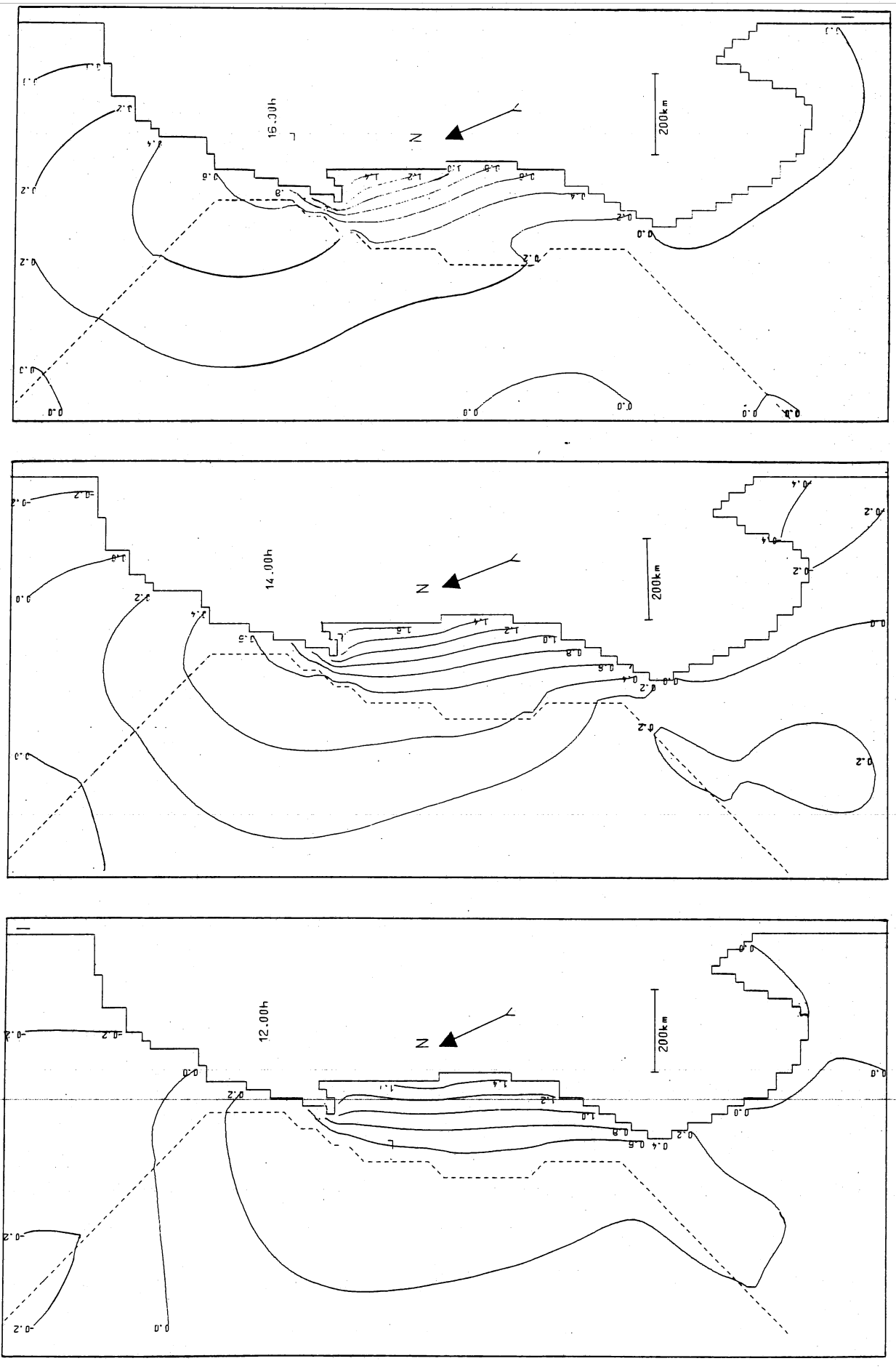


Fig. 7

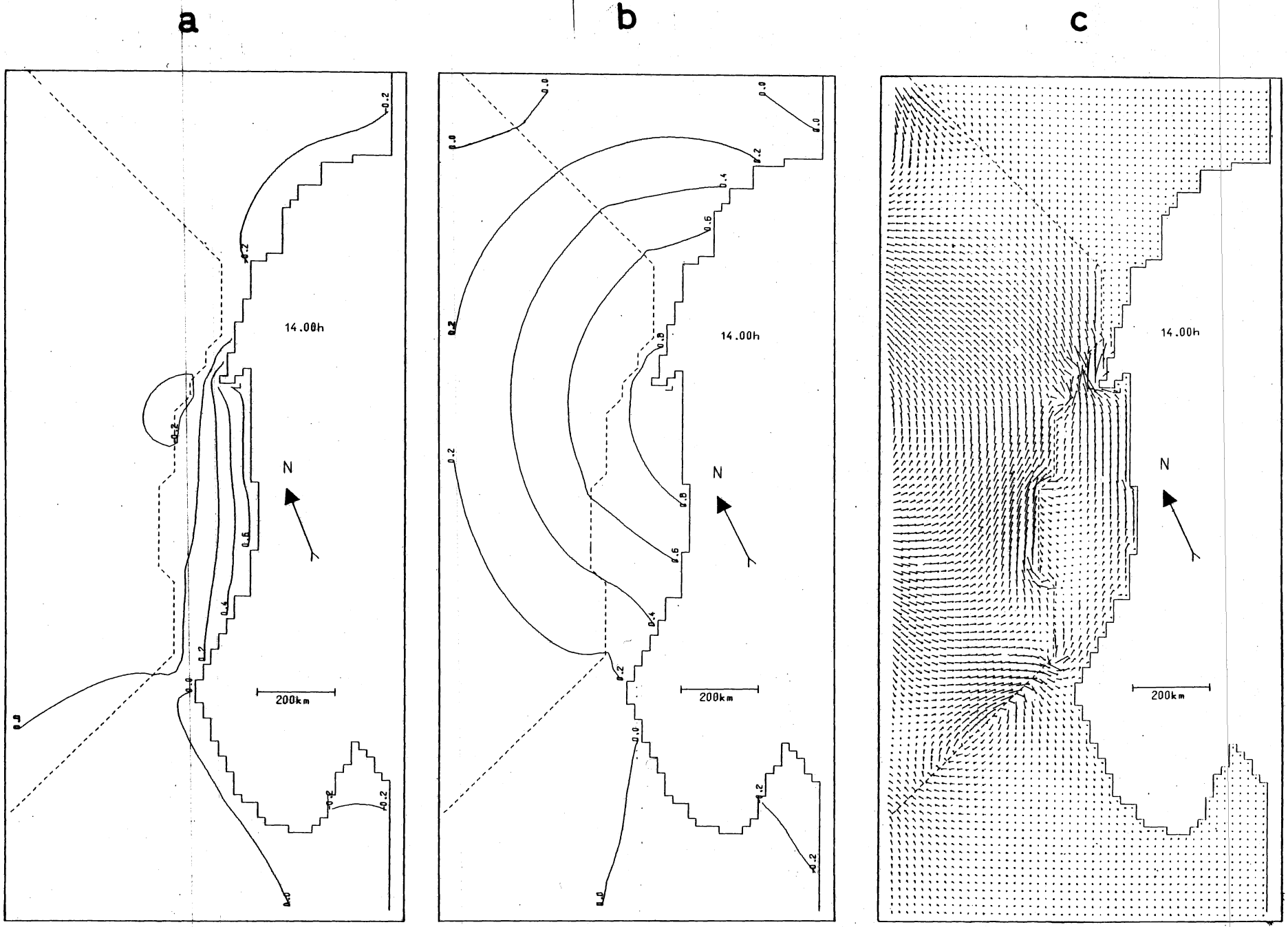


Fig. 8

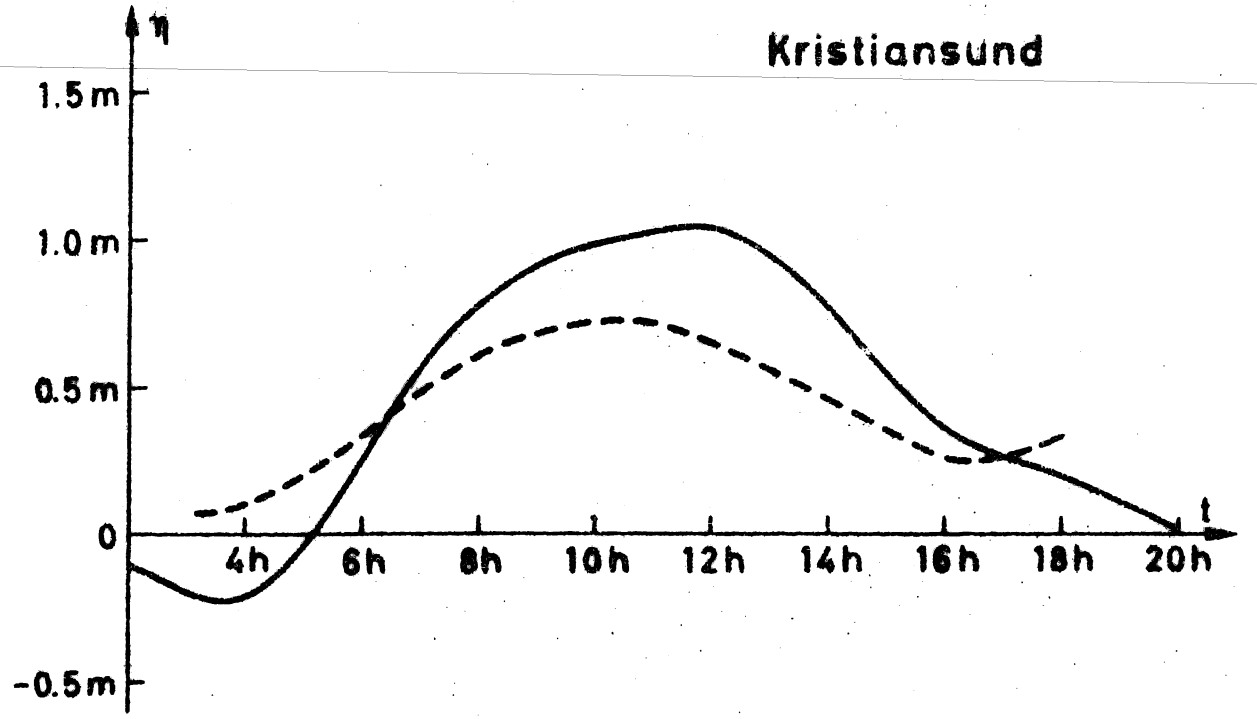
η
Kristiansund
1.5 m
1.0 m
0.5 m
0
-0.5 m
4h
6h
8h
10h
12h
14h
16h
18h
20h
t

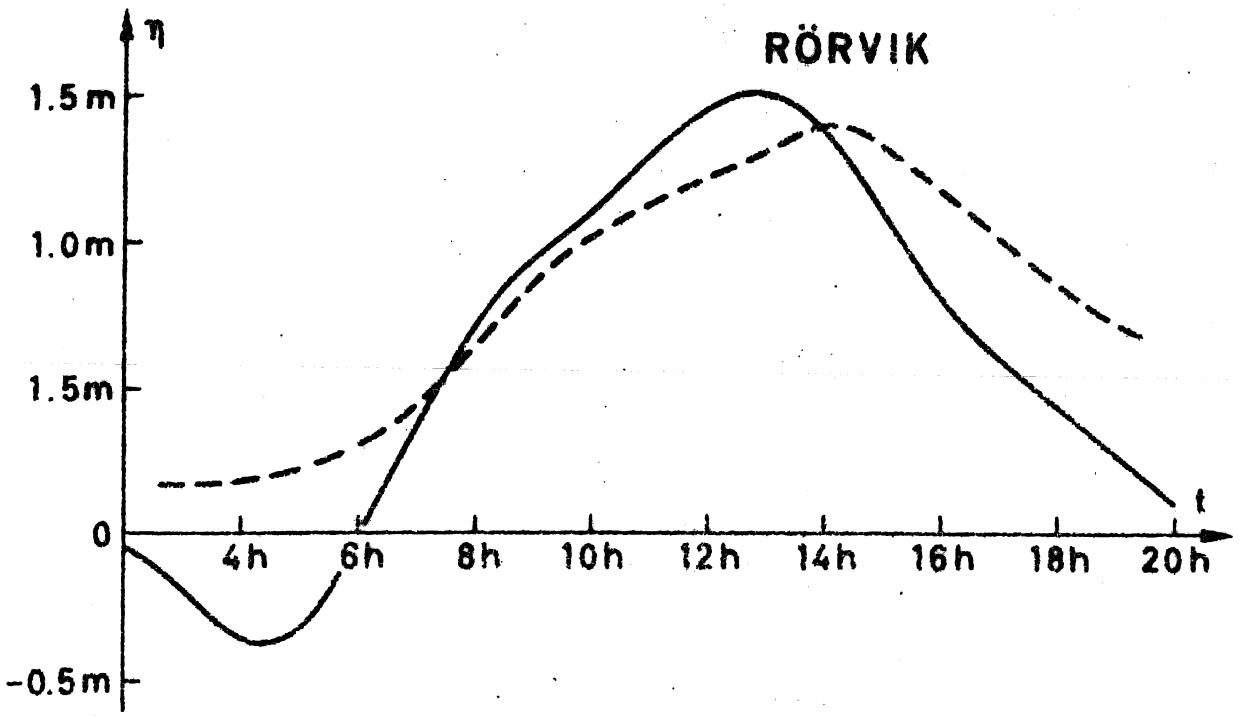
η
RÖRVIK
1.5 m
1.0 m
1.5m
0
-0.5 m
4h
6h
8h
10h
12h
14h
16h
18h
20h
t

Fig. 9